EFDA–JET–CP(12)05/01

T. Craciunescu, V. Kiptily, A. Murari, I. Tiseanu, V. Zoita
and JET EFDA contributors

Sparse Image Representation for JET Neutron and Gamma Tomography

Sparse Image Representation for JET Neutron and Gamma Tomography

T. Craciunescu[1], V. Kiptily[2], A. Murari[3], I. Tiseanu[1], V. Zoita[1]
and JET EFDA contributors*

JET-EFDA, Culham Science Centre, OX14 3DB, Abingdon, UK

[1]EURATOM-MEdC Association, Institute for Laser, Plasma and Radiation Physics, Bucharest, Romania
[2]EURATOM-CCFE Fusion Association, Culham Science Centre, OX14 3DB, Abingdon, OXON, UK
[3]Consorzio RFX, Associazione EURATOM-ENEA per la Fusione, Padova, Italy
** See annex of F. Romanelli et al, "Overview of JET Results",*
(23rd IAEA Fusion Energy Conference, Daejon, Republic of Korea (2010)).

Preprint of Paper to be submitted for publication in Proceedings of the
27th Symposium on Fusion Technology (SOFT), Liege, Belgium
24th September 2012 - 28th September 2012

ABSTRACT
The JET gamma/neutron profile monitor plasma coverage of the emissive region enables tomographic reconstruction. However, due to the availability of only two projection angles and to the coarse sampling, tomography is a highly limited data set problem. A new reconstruction method, based on the sparse representation of the reconstructed image in an over-complete dictionary, has been developed and applied to JET neutron/gamma tomography. The method has been tested on JET experimental data and results concerning the reconstruction of DT emissivity profile are presented. The proposed method provides good reconstructions in terms of shapes and resolution and produces artifact free images.

1. INTRODUCTION
JET neutron profile monitor is a unique instrument among neutron diagnostics available on large fusion research facilities [1-2]. The profile monitor comprises two fan shaped multi-collimator cameras, with 10 channels in the horizontal camera and 9 channels in the vertical camera. Neighbour channels are 15-20cm apart and have a 7 cm width as they pass near the plasma centre. A schematic drawing of the JET neutron emission profile monitor, showing the 19 lines of sight, is presented in Fig.1. Each line of sight is equipped with a set of detectors and associate electronics for simultaneous measurements of the 2.5MeV D-D neutrons, 14 MeV D-T neutrons and γ -rays. The collimation can be adjusted by use of two pairs of rotatable steel cylinders. The size of the collimation can modify the count rates in the detectors by a factor of 20. The instrument has currently a time resolution of 10ms.

The plasma coverage determined by the 19 lines of sight can be used for neutron or γ-ray tomography. It ensures a 2D arrangement for measurements and distribution determination. The 2D slice is located in the plane defined by the major torus radius (R) and the major torus axis (Z). The thickness of the plasma slice along the toroidal direction, determined by the collimation system, is approximately 75 mm. However, the existence of only two views (projections in tomographic terms) and the coarse sampling in each projection lead to a highly limited data set tomographic problem. Special algorithms which are suitable and specific to the machine and to its constraints, allowing effective tomography from the available limited data, are needed. A number of valuable approaches were developed in the past for tomographic reconstruction of the two-dimensional neutron and gamma emissivity on JET. Ingesson et al. [3] applied a constrained optimization method that uses anisotropic smoothness on flux surfaces as objective function and measurements as constraints.

This method, initially developed for soft X-ray tomography on JET, was applied to both γ-ray and neutron tomography (see e.g. Refs. 4-5). A reconstruction method based on the Tikhonov regularisation constrained to Minimum Fisher information was reported in Ref.6. Recently, the stability and speed of this method were improved by introducing a regularization matrix enforcing preferential emissivity smoothness along magnetic flux surfaces [7]. A reconstruction method based on the maximum likelihood principle proved to provide good reconstructions in terms of shapes and resolution [8]. The method uses a smoothing operator, defined as median filtering along the magnetic contour lines. Based on a neutron emissivity parametric model, Ronchi et al [9] uses a neural network in order to obtain tomographic reconstruction of neutron emissivity at JET.

The aim of this paper is to prove that accurate tomographic reconstructions can be obtained by using a sparse representation of the reconstructed image in an over-complete dictionary. The sparse image representation technique has lead, in the last years, to significantly improved results in signal, image, and video processing (see e.g. the pioneering work of Elad et al. [10] and Mairal et al. [11]). Significant results were reported recently also for tomography [12] in case of limited data for medical dental application (200×200 image, 23 projections uniformly distributed over approximately the full 180^{o}). JET neutron/gamma camera require to solve a more difficult problem, due to the scarcity of the available data: JET neutron profile monitor system has only two fairly coarse views of the plasma with a total of 19 projection bins.

2. METHODS

2.1 THE TOMOGRAPHIC PROBLEM

In 2-D tomography systems, measurements are taken along lines of sight, and can essentially be represented by line integrals; i.e. the measurement p is given by straight line integrals of the emissivity $f\,(x,y)$, where x and y are Cartesian coordinates of the plane. In a discretized representation, the tomographic problem can be formulated by the the relation:

$$p_k = \sum_{i=1}^{N_p} w_{ik} f_i, \quad k = 1,..., N_d \tag{1}$$

where f is the neutron/gamma emissivity function and N_p and N_d are the numbers of pixels and detectors, respectively. The projection matrix element w_{ik} represents the proportion of the emission f_i from pixel i, accumulated in detector k. Obviously, even with exact data constraints, this inversion cannot be uniquely performed when there are fewer data than pixels, as is generally the case in plasma tomography.

2.2 IMAGE SPARSE REPRESENTATION

The signal sparse representation problem consists of finding the optimal overcomplete dictionary that leads to the lowest reconstruction error given a fixed sparsity factor L (number of coefficients in the representation). The dictionary contains prototype atom-signals and the signals are described by sparse linear combinations of these atoms. The dictionary can be a fixed, general one (DCT, wavelet, curvelets, etc), or it can be adapted to suit the application domain. The reconstructive dictionary $D \in R^{N \times K}$ (N is the number of pixels in the image and K is the total number of atoms in the dictionary) is learned adaptively from the data such that the respective decomposition α_l is sparse (i.e., no more than L non-zero elements), by solving the optimization problem:

$$\{\alpha, D, f\} = argmin_{\alpha,D,g} \left\{ \underbrace{\Sigma_{j=1}^{M} \|g_j - D\alpha_j\|_2}_{image\ reconstruction} + \underbrace{\lambda\Sigma_{l=1}^{L} \|\alpha_l\|_0}_{sparsity} \right\} \tag{2}$$

where λ is a regularisation parameter. Since images are usually large, the decomposition is implemented on overlapping image patches $g_j = P_j f$ instead of the whole image f (P_j is the operator which extracts a specific patch g_j from the image f; M is the total number of patches). The patches are written as column vectors. The first term of the objective function measures the signal reconstruction error while the second one measures the signal sparsity.

2.3 THE RECONSTRUCTION METHOD

The tomographic reconstruction can be performed by reformulating (1) as an energy minimisation problem:

$$f = argmin_f \|Wf - p\|_2^2 \tag{3}$$

At the same time the image to be reconstructed f can be represented as a linear combination of a "few" atoms from a reconstructive dictionary D.

The unknown image f can be retrieved by minimising the following objective function:

$$\{\alpha, D, f\} = argmin_{\alpha,D,f} \left\{ \underbrace{\gamma \|f - p\|_2^2}_{tomographic\ reconstruction} + \underbrace{\lambda\Sigma_{j=1}^{M} \|\alpha_j\|_0}_{sparsity} + \underbrace{\lambda\Sigma_{j=1}^{M} \|g_j - D\alpha_j\|_2}_{sparsity} + \Omega_{smoothing \times f} \right\} \tag{4}$$

where γ is a regularisation term which controls the balance between the tomographic reconstruction and the image reconstruction from the overcomplete dictionary.

The last term in (4) is a regularization term, introducing a smoothness assumption in order to compensate for the lack of experimental information. As the tomographic problem is highly undetermined, the reconstruction algorithm can lead to a solution which satisfies Eq.(3) but it has no physical meaning and may result in wrong interpretations. Therefore *a priori* information about the expected emission profile can be introduced. Most of the methods developed for JET neutron/gamma cameras use a smoothness assumption so that the tomographic reconstruction searches for the emissivity distribution that is constant on magnetic flux surfaces. Some of them assume also a gentle variation in the radial direction. In our approach the smoothing operator is implemented as one-dimensional median filtering, using a sliding window which moves on the magnetic contour lines [8]:

$$f_i^{smooth} = \sum_{\substack{j=-W_{med} \\ W_{med} \in L_k}}^{j=W_{med}} m_{ij} f_j \tag{5}$$

m_{ij} is the matrix which defines the window-based median filter, w_{mad} is half of the width of the filtering window and L_k designates a close magnetic contour line.

3. IMPLEMENTATION AND RESULTS

The minimisation problem formulated by the objective function (4) is characterised by a high computational cost. It requires to solve the tomographic reconstruction as a chi-square problem together with the retrieval of the overcomplete dictionary and of the image representation in terms of its elements.

Recent results proved that learning non-parametric dictionaries simultaneously with the image representation provide improved results. However a large computational effort would be saved in case of using a pre-defined dictionary. A compromise between these two contradictory requirements can be obtained by using a priory information specific to JET neutron/gamma tomography. Therefore the dictionary D has been derived from a set of 50 already existent tomographic reconstructions which encompass most of shapes existent in this kind of tomography. These reconstructions have been obtained using the maximum likelihood (ML) tomographic method, described in Ref.8. In principle reconstructions derived with any tomographic method can be used for obtaining D. The ML method has the advantage to use the same smoothing technique (Eq.5) as in the present approach, so it represents a consistent choice. Once obtained, the dictionary D is used, unchanged, for all the tomographic reconstructions performed with the method introduced in this paper.

The ML reconstructions are represented as 38×70 pixels images. A collection of 250 random patches of the size of 8×8 pixels were randomly chosen for minimising the objective function in Eq.2. We used a dictionary of size $K = 256$ and a sparsity factor $K = 6$. The learned dictionary is presented in Fig.2. The minimisation of Eq.2 starts with random patches as a first guess of the dictionary elements and it was performed using the MATLAB implementation of the K-SVD algorithm [13]. K-SVD is a popular and practical algorithm which generalizes the K-means clustering process, solving a similar, but constrained problem.

After deriving the dictionary D, an iterative procedure is followed. This procedure allows, at each stage, the alternative minimisation of the tomographic reconstruction term, smoothing and sparse representation.

Due to the extreme scarcity of the experimental data, inherent in the neutron/gamma JET tomographic geometry, the Radon inversion does not provide a valid rough solution for the tomographic reconstruction. Therefore an initial solution f_0 with random values was chosen. The experimental projections have been transformed by resampling, using spline interpolation. Projection resampling implies the introducing of virtual lines of sight which ensures an improved coverage of the reconstruction domain. Resampling was performed so that the size of the synthesized signals is four times the initial one. The tomographic reconstruction term in Eq.4 was minimised as a chi-square problem, using the MATLAB *fminsearch* function which uses the Nelder-Mead simplex algorithm as described in Lagarias et al. [14]. After N_{iter}^{tomo} iterations, the algorithm switches to smoothing which is performed using Eq. 5 and a sliding window set at 1/10 of the size of the vector describing the magnetic contour line.

During the coding stage, the sparse decomposition is carried out with respect to $\{\alpha j\}_{j-1,...,1}$, based on the dictionary *D*. The Orthogonal Matching Pursuit (OMP) algorithm [15] represents an efficient tool for the iterative decomposition process. Given a fixed dictionary, OMP will first find the one atom that has the biggest inner product with the signal, and then subtract the contribution due to that atom, and repeat the process until the signal is satisfactorily decomposed.

A number of 80÷100 iterations of the procedure which alternates between tomographic reconstruction, smoothing and sparse representation are necessary, depending on the emissivity shapes in the reconstruction. For the experiments presented in this paper we have used a regularisation parameter $\gamma = 1.2$.

Representative results are presented in Fig.3. In order to evaluate the performance of the method, the results are presented together with those provided by Ingesson et al. method [16], which is used here as a reference method and together with the ML reconstructions. The results have been obtained for the application of the method to JET experimental data corresponding to an experiment with T-puff in the deuterium plasma. The "*banana*" distribution (Fig.3, top row) corresponds to an experiment where the DT-neutron emission was measured in the ohmic deuterium discharge during the off-axis injection of the T neutral beam. The reconstruction of a combined "*peak plus banana*" distribution (Fig.3, bottom row) reveals the emissivity shape just after the T-puff in the same discharge, when the tritons had only partly penetrated into the plasma core from the periphery.

The results prove that the method is able to retrieve highly sophisticated structures in the emissive distribution for this kind of tomography. The method provides good results in terms of shapes and resolution. The quality of the reconstruction is improved with respect to that provided by the ML method which was used for deriving the overcomplete dictionary.

CONCLUSION

We show in this paper that a sparse image representation principle can be successfully used for retrieving emissivity distributions in case of JET neutron/gamma tomography. *A priori* information is used in order to solve the highly undetermined tomographic problem. An overcomplete dictionary for the sparse representation is derived from a set of already existent tomographic reconstructions which encompass most of the possible shapes existent in this kind of tomography. Smoothing along magnetic contour lines is also used for additional regularization. The proposed method provides good reconstructions in terms of shapes and resolution. Further work will be dedicated to investigating the possibility of an implementation compatible with inter-shot analysis.

ACKNOWLEDGMENTS
This work, supported by the European Communities under the contract of Association between EURATOM and MEdC, CCFE, ENEA, was carried out under the framework of the European Fusion Development Agreement. The views and opinions expressed herein do not necessarily reflect those of the European Commission.

REFERENCES
[1]. J.M. Adams et al., Nuclear Instruments and Methods A **329**, 277 (1993).
[1]. O.N. Jarvis et al., F.B.Marcus, G.J. Sadler, Fusion Engineering and Design **34–35**, 59 (1997) 59.
[1]. L.C. Ingesson, et al., Nuclear Fusion, **38**, 1675 (1998).
[1]. V.G. Kiptily et al., Nuclear Fusion **49**, 065030 (2009).
[1]. K.D. Zastrow, et al., Plasma Physics and Controlled Fusion **46**, B255 (2004).
[1]. G. Bonheure, et al., Nuclear Fusion **46**, 725 (2006).
[1]. M. Odstrcil, et al., to be published in Nucl. Instrum. Methods Phys. Res. A. **686**, 156 (2012).
[1]. T. Craciunescu, et al., Nuclear Inst. and Methods in Physics Research, A, **605**, 373 (2009).
[1]. E. Ronchi, et al., Nucl. Nuclear Instruments Physics Results A **613**, 295 (2010).
[1]. M. Elad, et al., IEEE Transaction on Image Processing, **15-12**, 3736 (2006).
[1]. J. Mairal, et al., Advances Neural Information Processing Systems, 2008. Vancouver. Canada.
[1]. H.Y. Liao, et al., IEEE International Symposium on Biomedical Imaging, pp. 1375-1378, Paris, France, 2008.
[1]. M. Elad, M. Aharon, F. Bruckstein, K-SVD MATLAB Package, *http://www.cs.technion.ac.il/~elad/software/*.
[1]. J.C. Lagarias, et al., SIAM Journal of Optimization, **9-1**, 112 (1998).
[1]. S. Mallat et al., IEEE Transactions on Signal Processing, **41**, 3397 (1993).
[1]. V. Kiptily, Library of 14MeV tomography reconstructions, *http://users.jet.efda.org/pages/dt-task-force/pages/TTE_AlphaSources_Kiptily/AlphaSources_Table.htm*.

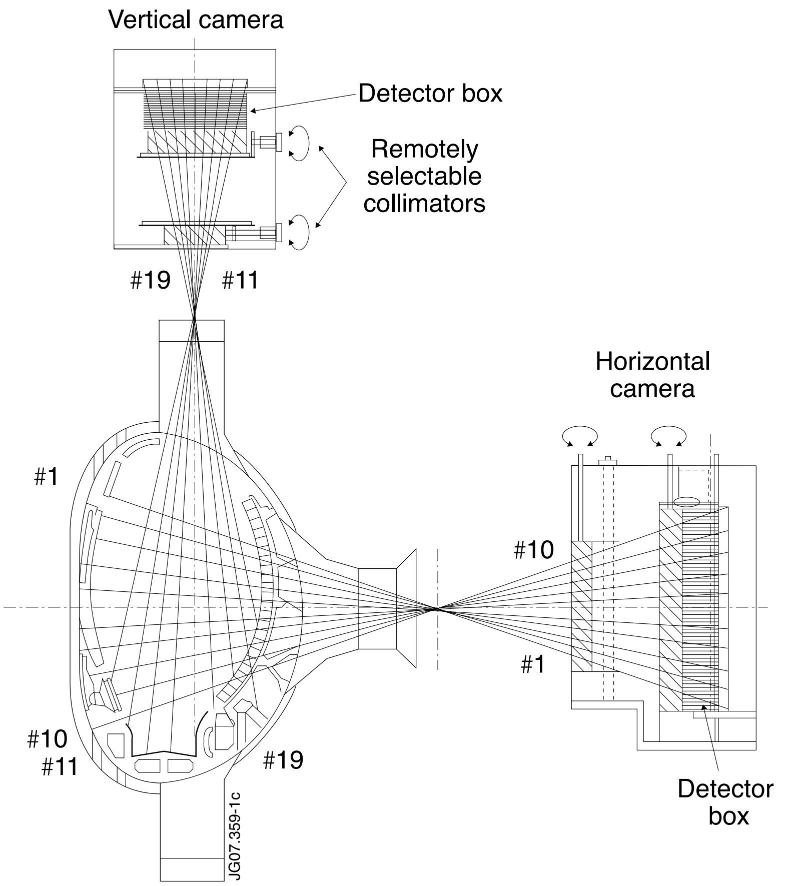

Figure 1: Schematic view of JET neutron emission profile monitor showing the lines of sight.

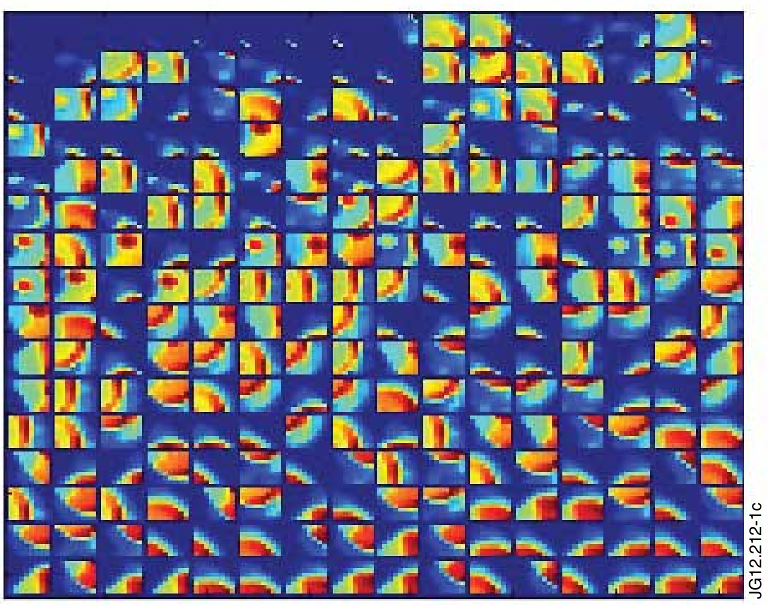

Figure 2: The dictionary D learned from 50 tomographic reconstructions obtained using the ML method. This dictionary was used as an initial guess for solving Eq.4.

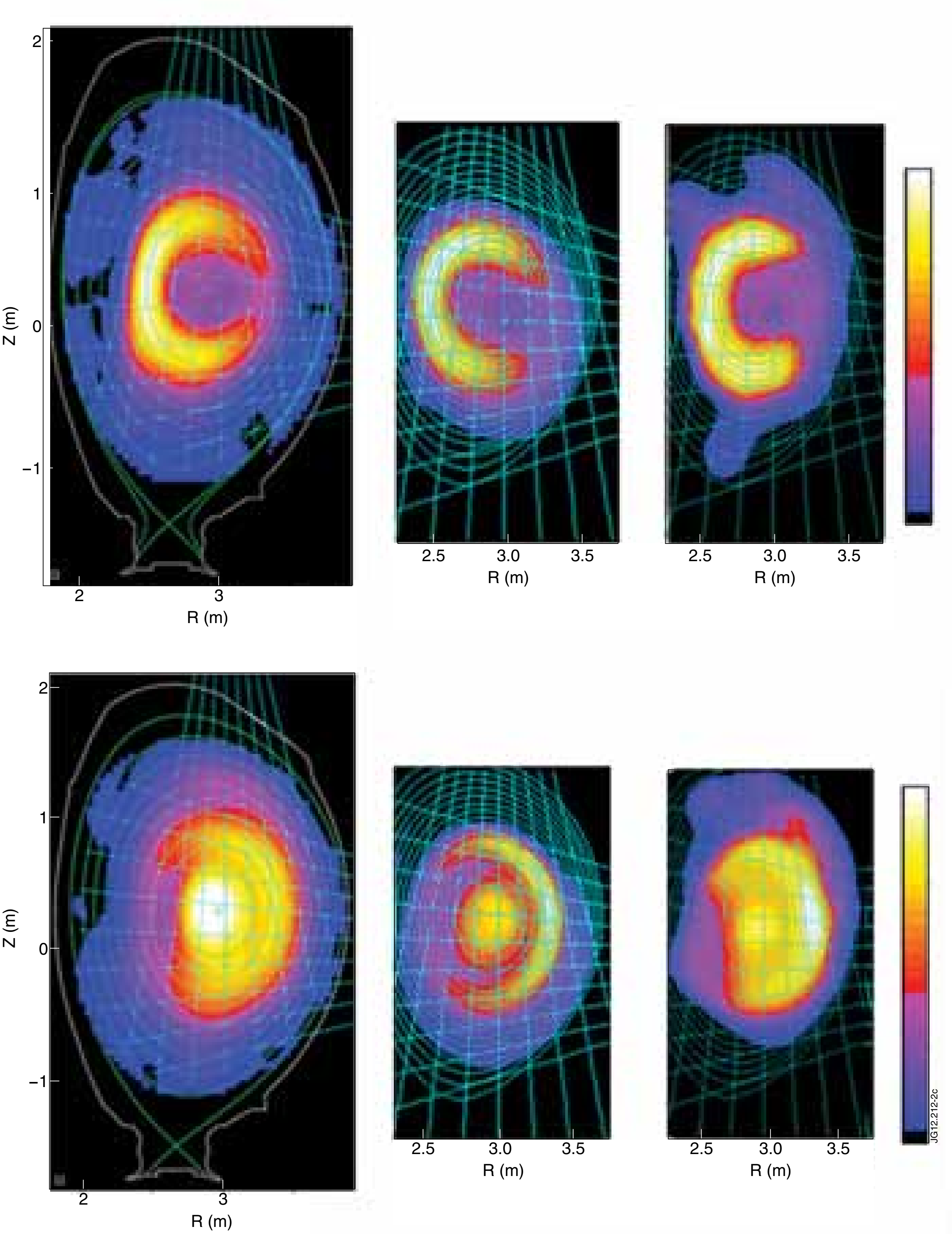

Figure 3: Comparison between DT-neutron emissivity profile reconstructions. The left column shows the reconstructions obtained using the reference method [16]; the middle column presents the reconstructions obtained using the ML method, which was used for deriving the overcomplete dictionary; the right column illustrates the results provided by the method introduced in this paper. Top row shows the "banana" profile distribution corresponding to an experiment where the DT-neutron emission was measured in the ohmic deuterium discharge during the off-axis injection of the T neutral beam—Pulse No: 61237 at 6.22–6.27s (top row); Bottom row shows the "peak plus banana" profile distribution recorded just after the T-puff, when tritons partly penetrated into the plasma core from the periphery—Pulse No: 61132 at 22.67s (bottom row).